

# Experimental studies of thin-walled aircraft structures

## Badania eksperymentalne zestawu cienkościennych konstrukcji lotniczych

PAWEŁ BAŁON  
EDWARD REJMAN  
BARTŁOMIEJ KIEŁBASA  
ROBERT SMUSZ  
GRZEGORZ SZELIGA \*

DOI: <https://doi.org/10.17814/mechanik.2022.10.16>

Contemporary aircraft structures, and especially their load-bearing structures, are made almost exclusively as thin-walled structures, which perfectly meet the postulate of minimizing the weight of the structure. While local loss of roofing stability is acceptable under operational load conditions, exceeding the critical load limits of structural elements (frames, stringers) is practically tantamount to the destruction of the structure. The effectiveness of these ideas is influenced by the development of science about materials, processing, and machining processes, as well as the continuous improvement of technological processes. These disciplines allow for the construction of complex, geometrically integral structures that create opportunities not only for a more rational use of material characteristics, but also by their appropriate shaping, significantly increasing the mechanical properties of the supporting structure. The most important advantage in favor of the use of integral systems is economic efficiency, gained by eliminating or limiting assembly operations. Densely ribbed roofing elements belong to the category of load-bearing structure elements which, by reducing the weight which they must support, increase the strength parameters of the load-bearing structure. By reducing the thickness of the coating and, at the same time, introducing sufficiently dense stiffening longitudinal elements, it is possible to obtain a structure with significantly higher critical load values, and consequently a more favorable distribution of gradients and stress levels, which translates directly to an increase in fatigue life. The use of new technologies requires research for evidence purposes, showing that structures manufactured in this way are as safe as those manufactured using conventional methods. For this purpose, the authors conducted tests of the selected structure and performed FEM and experimental verification on the test stand. The results of the tests showed positive results, which confirmed that the method of manufacturing integral structures meets even the stringent requirements set by aviation.

**KEYWORDS:** HSM, HSC, high speed milling, high speed cutting, experimental verification, MES

Współczesne konstrukcje lotnicze, a zwłaszcza konstrukcje nośne, wykonywane są niemal wyłącznie jako struktury cienkościenne, co doskonale realizuje wymóg minimalizacji masy samolotów. O ile miejscowa utrata stateczności pokrycia jest dopuszczalna w warunkach obciążenia eksploatacyjnego, o tyle przekroczenie granicznych obciążeń krytycznych elementów konstrukcyjnych (wreęg, podłużnic) jest praktycznie równoznaczne ze zniszczeniem konstrukcji. Skuteczność rozwiązań konstrukcyjnych jest zapewniana przez rozwój nauki o materiałach i procesach obróbki oraz ciągłe doskonalenie procesów technologicznych. To pozwala na projektowanie złożonych, geometrycznie integralnych konstrukcji, które umożliwiają bardziej racjonalne wykorzystanie właściwości materiałów, a także – dzięki ich odpowiedniemu kształtowaniu – znaczne ulepszenie właściwości mechanicznych konstrukcji nośnych. Najważniejszą zaletą przemawiającą za zastosowaniem systemów integralnych jest efektywność ekonomiczna, uzyskana poprzez wyeliminowanie lub ograniczenie montażu. Gęsto uźebrowane komponenty poprzez zmniejszenie ciężaru, jaki muszą przenosić, poprawiają parametry wytrzymałościowe konstrukcji nośnej. Zmniejszając grubość powłoki i jednocześnie wprowadzając odpowiednio gęsto podłużne elementy usztywniające, można uzyskać konstrukcje o znacznie wyższych dopuszczalnych wartościach obciążeń krytycznych, a w konsekwencji korzystniejszym rozkładzie gradientów i poziomów naprężeń. Przekłada się to bezpośrednio na zwiększenie trwałości zmęczeniowej. Zastosowanie nowych technologii wymaga przeprowadzenia badań wykazujących, że konstrukcje wytworzone w ten sposób są równie bezpieczne, jak te wytwarzane metodami konwencjonalnymi. W tym celu autorzy przeprowadzili badania wybranej konstrukcji lotniczej oraz weryfikację numeryczną MES i eksperymentalną na stanowisku badawczym. Wyniki testów potwierdziły, że sposób wytwarzania konstrukcji integralnych spełnia nawet rygorystyczne wymagania stawiane przez branżę lotniczą.

**SŁOWA KLUCZOWE:** HSM, HSC, frezowanie z dużą prędkością, cięcie z dużą prędkością, weryfikacja eksperymentalna, MES

\* Dr inż. Paweł Bałon – balonpawel@gmail.com, <https://orcid.org/0000-0003-3136-7908> – AGH University of Science and Technology, Kraków, Poland; SZEL-TECH, Mielec, Poland  
Dr inż. Edward Rejman – erejman@prz.edu.pl, <https://orcid.org/0000-0003-4716-7613> – Rzeszów University of Technology, Rzeszów, Poland; SZEL-TECH, Mielec, Poland  
Mgr inż. Bartłomiej Kiełbasa – bartek.kielbasa@gmail.com, <https://orcid.org/0000-0002-3116-2251> – SZEL-TECH, Mielec, Poland  
Dr hab. inż. Robert Smusz – robsmusz@gmail.com, <https://orcid.org/0000-0001-7369-1162> – Rzeszów University of Technology, Rzeszów, Poland; SZEL-TECH, Mielec, Poland  
Grzegorz Szeliga – g.szeliga@szel-tech.com – SZEL-TECH, Mielec, Poland

**TABLE I. Chemical composition of aluminum alloys 7075 and 7050 [7]**

	Mg	Mn	Fe	Si	Cu	Zn	Cr	Ti	Zr + Ti	Other	Other all	Al
Alloy 7075	2.10 ÷ 2.90	≤ 0.30	≤ 0.50	≤ 0.40	1.20 ÷ 2.00	5.10 ÷ 6.10	0.18 ÷ 0.28	≤ 0.20	≤ 0.25	≤ 0.05	≤ 0.15	rest
Alloy 7050	1.9 ~ 2.6	0.1	0.15	0.12	2.0 ~ 2.6	5.7 ~ 6.7	0.04	0.06	0.08 ~ 0.15	0.15	≤ 0.15	rest

## Introduction

Aircraft structures require three basic criteria to be met: adequate strength, stiffness, and minimal structure weight. These features define the cross-sectional areas down to the smallest dimensions of the thickness of the members. Local buckling of roofing structural members is acceptable in many load cases, while exceeding the critical load levels of members such as frames, beams or stringers causes structural failure. The development of materials science and technological processes allows for the production of geometrically complex integral structures. The most important advantage of using integral structures is the cost savings derived from the reduction or elimination of assembly operations. It is possible to obtain structures with much higher critical loads by reducing the thickness of the coating and using properly spaced ones and stiffened longitudinal members. The growing interest in high speed machining, especially in the aerospace industry, is associated with a number of benefits obtained after the implementation of this technology. High speed machining (HSM) is currently one of the key machining technologies developed and used in the aerospace industry. The factor that distinguishes HSM from other milling techniques is the choice of cutting parameters: depth of cut, feed, and cutting speed to ensure good quality and accuracy of the machined surface and, at the same time, high machining efficiency to shorten the manufacturing process of integral parts [1, 2, 4, 9].

By introducing HSM, it is possible to make very complex, integral aircraft parts from a rectangular blank with thin walls. Currently, in designing the structure of an aircraft, the aim is to make it consist mainly of integral elements which, until recently, have been produced by joining components using welding, fusion, or riveting technology processes. This group of integral elements includes parts such as ribs, stringers, girders, and frames, as well as fuselage and wing coverings. After machining, these parts are assembled into larger assemblies. The main purpose of the applied procedures, apart from meeting the functionality criterion, is to obtain the best possible strength-to-weight ratio of the structure. The use of high machining speeds enables the economical production of integral parts by reducing the machining time, but it also improves the quality of the machined surface (e.g., surface roughness, waviness, manufacturing tolerances). Due to the fact that the cutting forces in such a process are much lower than those used for conventional machining methods, this factor affects the displacement of the workpiece, and thus the accuracy of mapping the machined surfaces.

## Research of material for frames

The basic material for high-strength integral structures of aircraft structures are aluminum alloys EN AW-7050 and EN AW-7075 [7]. In the considered structure, alloy type 7075 was used, which is characterized by high strength properties, very good thermal conductivity, and medium corrosion resistance (tab. I). The alloy also shows very good machinability. The many properties offered by 7075 aluminum alloy make it a good choice for universal use in a variety of industries, especially in the aviation and transport industry, due to its high strength-to-weight ratio (i.e., high specific strength).

In order to assess the actual values of the strength properties of the alloy, tests were carried out on samples in the T6 state (supersaturated and artificially aged material) [5] (fig. 1, tab. II).

The actual material showed a much higher tensile strength than the data given in the standards [5]. An important piece of information is the placement of the sample in relation to its rolling direction.

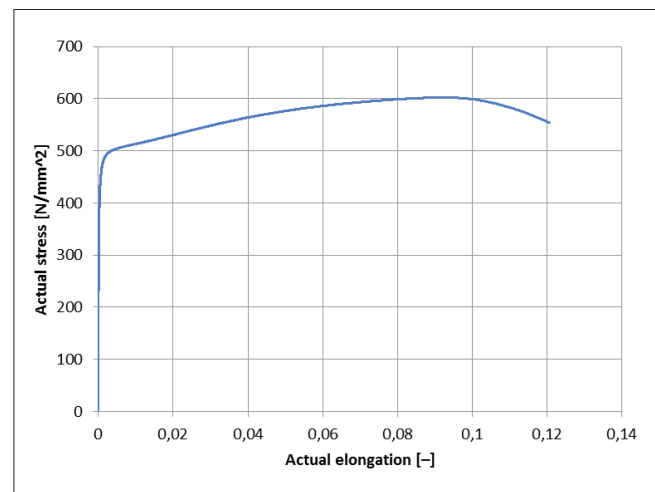


Fig. 1. Tensile diagram for samples made of the 7050 T6 Alloy

**TABLE II. Mechanical properties of samples made of alloy 7050**

	Sheet thickness			
	1.5 mm		1.6 mm	
	Rolling direction			
	0°	90°	0°	90°g
Hardness [HV1]	183	183	180	180
$R_m$ [MPa]	595	595	548	562

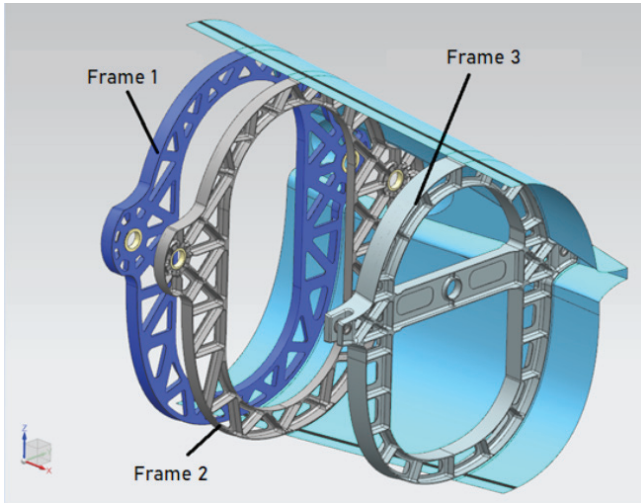


Fig. 2. Model of the tested structural unit composed of three frames and a covering

### Numerical analysis of the tested object

In order to implement the presented method of constructing aviation equipment in practice, a model of the fuselage part of the sailplane was made, in which metal cooperating frames were used with composite epoxy glass coating. The frames were glued into the covering section.

As a result, the object reproduces a fragment of the hull structure in a 1:1 scale, which is shown in figures 2–3. The cover material is epoxy-glass composite, while the frames are made of AW 7050 T-7451 aluminum alloy. For gluing, a two-component epoxy adhesive of the 3M DP490 Scotch-Weld type was used.

In order to perform the calculations, a computational grid was put on the object, which contained 10 mm CQUAD8 type elements (tab. III), using the MCID orientation method and the PCOMP format. Connection zones with other objects have been separated. LAYUPS zones were separated for the laminate layer arrangement in accordance with the covering lamination plan. The computational solver was the computing environment of the FEM engineering software. This analysis includes static tests under a torque load of up to 21 kNm.

The strength analysis was carried out by applying the forces  $F$  (fig. 6) from the value of +5 kN/–5 kN in

TABLE III. Characteristics of the FEM mesh of the facility

Total number of elements in the part	1 780 820
Total number of nodes in the part	3 384 272
Number of Rigid Link elements	14 292
Number of Quad8 elements	34 985
Number of Tetra10 elements	1 731 543
Minimum element label used	89 060
Maximum element label used	3 468 539
Minimum node label used	10
Maximum node label used	3 489 205

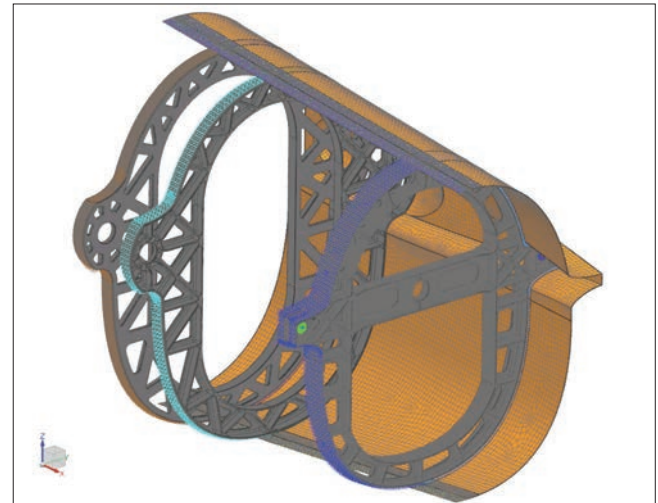


Fig. 3. Assembly model with a generated mesh for FEM calculations

steps of +5 kN/–5 kN until the Failure Index noticeably exceeded positive, which corresponds to structural damage. Failure index was calculated according to PlyFailure Theory Tsai-Wu (The Shear Stress for Bonding value was assumed to be 70 MPa). The results were developed for the resulting loads from the applied forces +5 kN/–5 kN, +10 kN/–10 kN, +15 kN/–15 kN, +20 kN/–20 kN, additionally, for research purposes, the design was verified with a computational force of +35 kN/–35 kN.

The FEM verification indicated the places where the stress concentration should be expected. When comparing the isolated assemblies (frame group 3/4), we can see that replacing them with assemblies in the HSM technology has development potential, due to the introduction of concentrated forces into the composite structure. They have a higher load-bearing capacity at a comparable weight. This is particularly evident in GFRP (glass fiber reinforced polymers) technology. By optimizing the shape of the points for introducing concentrated forces into the frames, which is easy to implement thanks to the HSM technology, even more favorable stress distributions can be obtained. For this

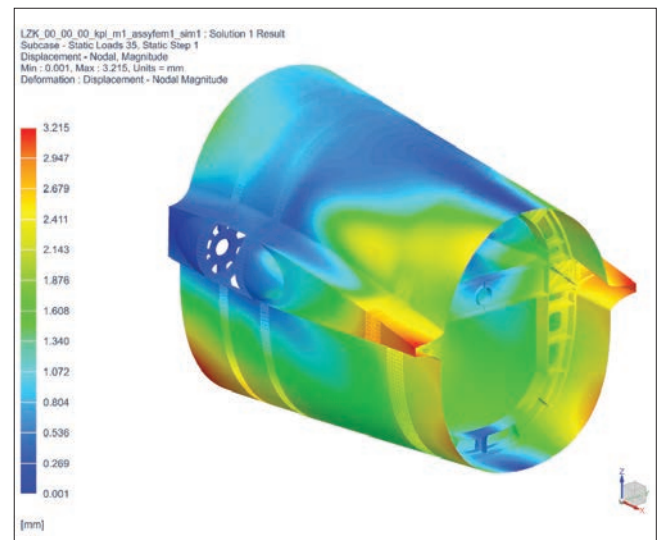


Fig. 4. The state of displacement in the modeled assembly under the load  $F = \pm 35$  kN

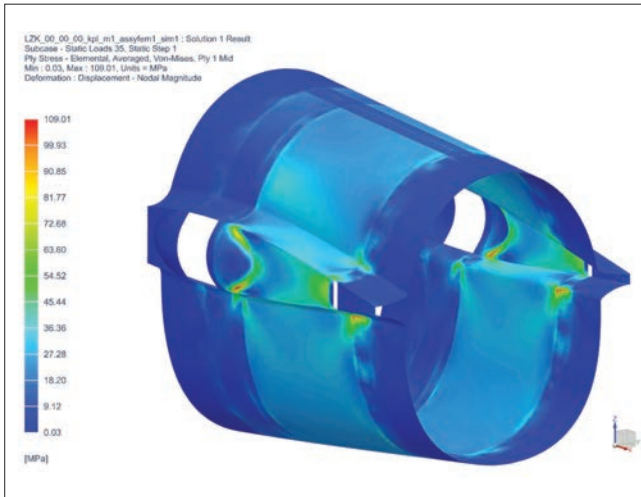


Fig. 5. The state of stress in the modeled assembly under the load  $F = \pm 35$  kN

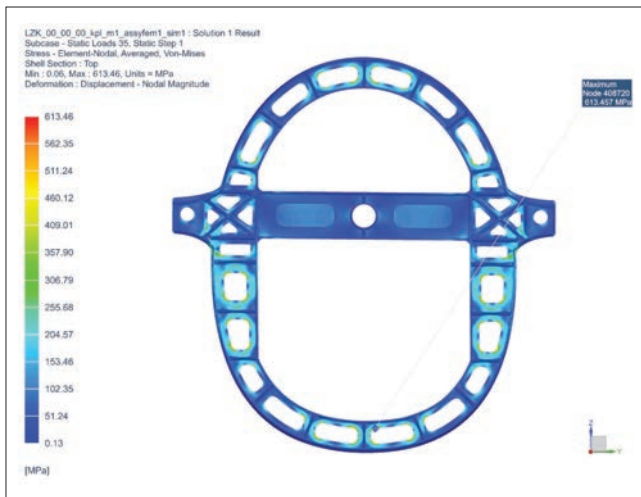


Fig. 6. The state of stress in frame 3 under the load  $F = \pm 35$  kN

purpose, it was necessary to correctly model the metal-composite connection and the metal frame nodes with the highest stresses, so as to obtain the lowest possible stress concentration during the experimental verification (i.e., testing the assembly with a twisting movement) [3, 6, 8].

### Strength test of the real structure

Before starting the tests, it was decided to combine the two trials into one cycle: Test A (structure load 100% of the nominal value) and Test B (breaking load). The design load (resulting from the load of this class of sailplanes) was  $F = 35$  kN. After exceeding the load of 35 kN on the loading cylinder, the test was continued, increasing the load until the structure was destroyed. The structure was twisted by applying vertical forces  $F$  of opposite turns to the point where the mounting pin passed through the frame 3 (fig. 7), allowing for the possibility of compensation for frictional forces and moments. The tested structure was fixed in a special equipment (fig. 8).

Parameters of the performed test:

- test temperature: 20°C;
- loading speed: 1.75 kN/min;

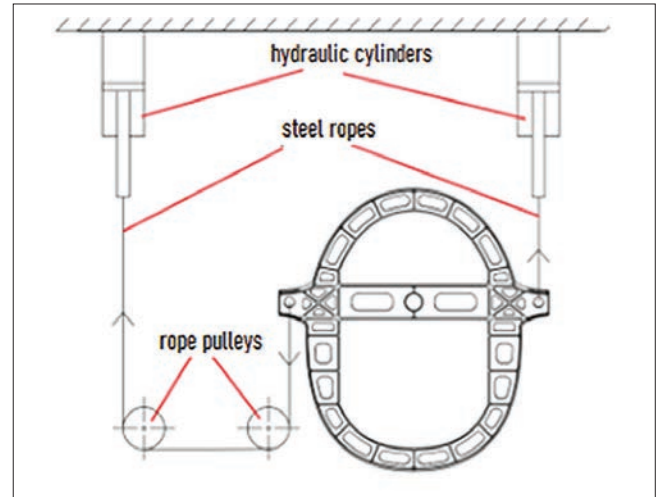


Fig. 7. Diagram of the loading system of the tested structure

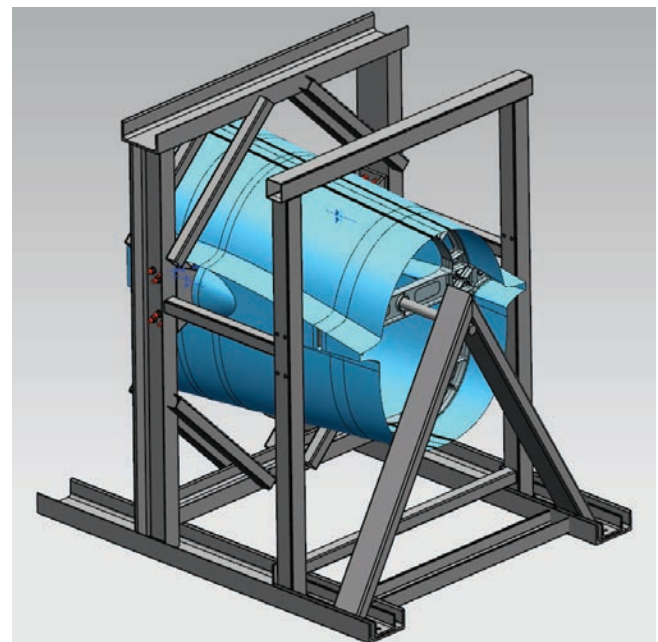


Fig. 8. View of the tested structure mounted in the equipment

- maximum level of loads implemented in the sample: 100% of the design load value;
- time of maintaining the load at a given level: minimum 15 seconds;
- measuring sensors used: 5 strain gauges of the type TFs-10/350, 1 strain gauge of the type TFrw-3/120.

### The course of the research process

Tests up to the calculation level of the loading force  $F = 35$  kN: the assumed speed of the load increase and the time of its operation at individual levels was maintained, the displacement of the force application points was recorded, the deformation values were recorded at the frame and covering measurement points (fig. 8). For the full design load, no visible damage to the laminate structure of the roofing and the frame walls, including any local loss of stability, was observed. The calculated shear stresses in the adhesive layer joining frame 3 to the coating amounted to  $t = 19$  MPa and were lower than the destructive stresses for this

**TABLE IV. Results of stress measurements at selected points of the frame**

Load per side [kN]	Strains ( $\epsilon$ ) and stresses ( $\sigma$ ) at measuring points									
	Strain gauge 1		Strain gauge 2		Strain gauge 3		Strain gauge 4		Strain gauge 5	
	$\epsilon$ [-]	$\sigma$ [MPa]	$\epsilon$ [-]	$\sigma$ [MPa]	$\epsilon$ [-]	$\sigma$ [MPa]	$\epsilon$ [-]	$\sigma$ [MPa]	$\epsilon$ [-]	$\sigma$ [MPa]
3.5	$1.12 \cdot 10^{-4}$	8.05	$9.84 \cdot 10^{-6}$	0.71	$2.57 \cdot 10^{-5}$	1.84	$5.25 \cdot 10^{-5}$	3.77	$5.71 \cdot 10^{-5}$	4.09
7.0	$2.21 \cdot 10^{-4}$	15.87	$1.92 \cdot 10^{-5}$	1.38	$5.19 \cdot 10^{-5}$	3.72	$1.06 \cdot 10^{-4}$	7.58	$1.19 \cdot 10^{-4}$	8.53
10.5	$3.29 \cdot 10^{-4}$	23.60	$2.81 \cdot 10^{-5}$	2.02	$7.91 \cdot 10^{-5}$	5.67	$1.61 \cdot 10^{-4}$	11.56	$1.82 \cdot 10^{-4}$	13.04
14.0	$4.36 \cdot 10^{-4}$	31.25	$3.73 \cdot 10^{-5}$	2.68	$1.06 \cdot 10^{-4}$	7.60	$2.17 \cdot 10^{-4}$	15.56	$2.46 \cdot 10^{-4}$	17.65
17.5	$5.46 \cdot 10^{-4}$	39.11	$4.66 \cdot 10^{-5}$	3.34	$1.34 \cdot 10^{-4}$	9.60	$2.62 \cdot 10^{-4}$	18.76	$3.08 \cdot 10^{-4}$	22.08
21.0	$6.55 \cdot 10^{-4}$	46.94	$5.59 \cdot 10^{-5}$	4.00	$1.61 \cdot 10^{-4}$	11.57	$3.09 \cdot 10^{-4}$	22.15	$3.70 \cdot 10^{-4}$	26.53
24.5	$7.64 \cdot 10^{-4}$	54.77	$6.55 \cdot 10^{-5}$	4.69	$1.89 \cdot 10^{-4}$	13.56	$3.56 \cdot 10^{-4}$	25.49	$4.32 \cdot 10^{-4}$	30.96
28.0	$8.74 \cdot 10^{-4}$	62.65	$7.44 \cdot 10^{-5}$	5.33	$2.17 \cdot 10^{-4}$	15.55	$4.00 \cdot 10^{-4}$	28.70	$4.92 \cdot 10^{-4}$	35.28
31.5	$9.83 \cdot 10^{-4}$	70.50	$8.34 \cdot 10^{-5}$	5.98	$2.44 \cdot 10^{-4}$	17.49	$4.46 \cdot 10^{-4}$	31.95	$5.52 \cdot 10^{-4}$	39.61
35.0	$1.09 \cdot 10^{-3}$	78.30	$9.25 \cdot 10^{-5}$	6.63	$2.71 \cdot 10^{-4}$	19.41	$4.92 \cdot 10^{-4}$	35.30	$6.12 \cdot 10^{-4}$	43.90

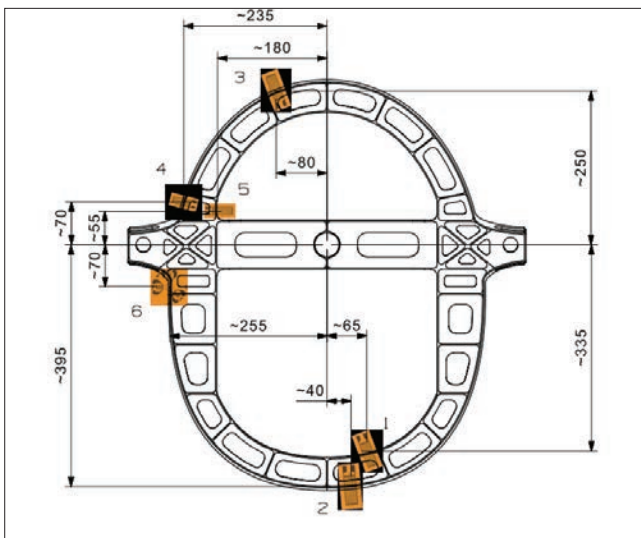


Fig. 9. Diagram of the arrangement of strain gauges on the frame 3

adhesive as determined by the authors in tests of overlap samples, amounting to  $t_{\max} = 22.3$  MPa.

After the end of the test according to variant A, the tests were continued in order to destroy the structure. Maintaining the test conditions, the load was increased until the first symptoms of structural damage appeared. This resulted in a characteristic click sound, which physically meant the destruction of the rib-cover junction. The failure occurred with the force loading the node equal to 54 kN, which corresponds to the value of 154% of the design loads. The calculated shear stresses in the adhesive layer amounted to  $t = 29$  MPa, and were greater than the sample destructive stress (according to our own experimental research), which confirms the correctness of the destruction of the adhesive. In the area where the strain

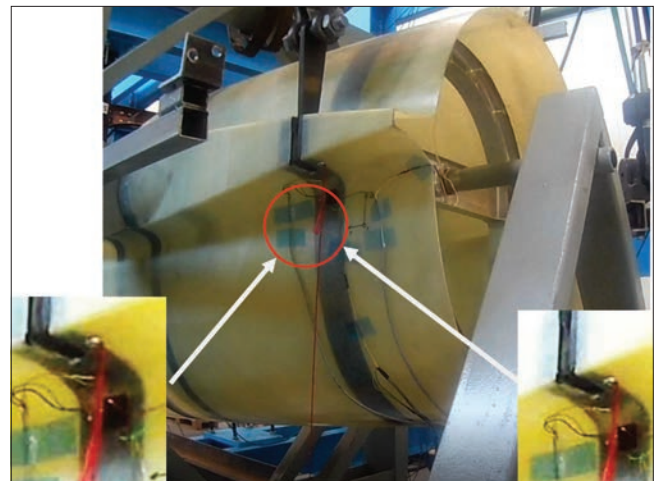


Fig. 10. View of damage to the laminate structure of the plating and a comparison of the states before and after the test (increased contrast and brightness in photos)

gauge rosette was located on the plating (measurement point 6), local whitening was observed, with an intensity increasing along with increased load, which indicated that the frames were detached from the hull plating (fig. 10). The measured stresses reduced in the coverage reached the value of  $\sigma_{\text{red}}$ , equal to 255.4 MPa under the design load.

## Conclusions

The tested structure retained its shape and physical properties in the full range of nominal loads. No cracks or delamination of the laminate structure, nor of the veneers, were observed. Permanent damage to the structure occurred at a breaking load corresponding to 154% of the value of the nominal loads. As a re-

sult of the destruction, the veneer was detached from the covering locally. However, this did not affect the geometrical form of the entire structure. The highest values of deformations and stresses were recorded on the rosette glued to the laminate covering, which is mainly related to the construction of this node resulting and local stress concentration. Particularly noteworthy is the fragment of the sheathing above the fitting, where the stress may reach values close to the limit values for the glass composite.

The use of metal frames allows for their dimensions to be reduced in relation to composite frames, especially in the places where concentrated forces are introduced. The lower stiffness of the version of the structural solution with the metal frame allows the stress to be distributed more efficiently over the entire frame, but this means much higher stresses on the roofing, which is an element structurally weaker than the metal frame, which may result in the skin tearing at higher load values and thus, the stress may reach values close to the limit values for the glass composite. The introduction of the HSM technology enables faster and cheaper production start-up and easier modification of the elements due to the reduction of the tooling necessary for their production in relation to the laminate elements. Metal elements made using the HSM technology, with a weight comparable to products made in other technologies, demonstrate a higher load capacity, especially in nodes loaded with concentrated forces.

In the exemplary solution, the fuselage structure segment with 7050 aluminum alloy frames had a weight 2.53 kg lower than the structure with epoxy-carbon composite frames, i.e. a 12,5% reduction in weight, which significantly affects the weight of the aircraft.

### Acknowledgements

**Badania zrealizowano w ramach projektu o nr RPPK.01.02.00 – 18 – 0002/20 – 00, pt. „Prace rozwojowe nad opracowaniem i wdrożeniem technologii wykonywania zespołów lotniczych o integralnej strukturze cienkościennej”, współfinansowanego ze środków Europejskiego Funduszu Rozwoju Regionalnego.**

### LITERATURA

- [1] Pilecki S. „*Lotnictwo i kosmonautyka*”. Warszawa: WKŁ (1978).
- [2] Galiński C. „*Wybrane zagadnienia konstrukcji samolotów*”. Warszawa: Oficyna Wydawnicza Politechniki Warszawskiej (2020).
- [3] Sibilski K. „*Mechanika w lotnictwie*”. T. II. Warszawa: Polskie Towarzystwo Mechaniki Teoretycznej i Stosowanej (2016).
- [4] Jemieliński K., Karolczak P., Subbotko R., Borkowski W., Rusiecki O. „*Nowoczesne procesy obróbki skrawaniem*”. Warszawa: PWN (2022).
- [5] Bijak-Żochowski M. „*Mechanika materiałów i konstrukcji*”. T. I. Warszawa: Oficyna Wydawnicza Politechniki Warszawskiej (2013).
- [6] Bijak-Żochowski M. „*Mechanika materiałów i konstrukcji*”. T. II. Warszawa: Oficyna Wydawnicza Politechniki Warszawskiej (2013).
- [7] PN-EN 573-3:1998. Aluminium i stopy aluminium – Skład chemiczny i rodzaje wyrobów przerobionych plastycznie – Skład chemiczny.
- [8] Kiełbasa B., Bałon P., Świątoniowski A., Szostak J. „Fatigue fracture analysis of composite plates with an elliptical hole”. *Strength of Materials*. 49, 4 (July, 2017): <https://doi.org/10.1007/s11223-017-9893-1>.
- [9] Bałon P., Rejman E., Kiełbasa B., Smusz R. “Using HSM technology in machining of thin-walled aircraft structures”. *Acta Mechanica et Automatica*. 16, 1 (2022): 27–33, <https://doi.org/10.2478/ama-2022-0004>. ■